Military Technical College
Kobry El-Kobbah
Cairo, Egypt

10th International Conference
On Aerospace Sciences&
Aviation Technology

A SMALL AIRCRAFT IN HAZARDOUS WAKE NEAR GROUND USING UNSTEADY VORTEX LATTICE METHOD

Saad M. Issa* and Abdulhamid A. Ghmmam**

ABSTRACT

The interaction between small aircraft and vortex system generated by another much larger aircraft is investigated. An aerodynamic model based on the modified unsteady vortex lattice method and the method of images was developed. A simple wake model can be developed using this vortex system.

The large aircraft represented by a large wing, while, the small aircraft represented by a small wing, were used in this study. Investigation was done for the small aircraft, as it is entering and flying parallel to the wake left by the larger aircraft near ground, during aircraft landing operation, with all aerodynamic surfaces assumed to be of zero thickness. The lateral position of the small wing with respect to the large wing center line is assumed to be variable. Changes in lift, drag, pitching moment and rolling moment coefficients, for the small aircraft, are calculated and presented for deferent cases of study.

A case study shows that, as the small aircraft enters the wake left by a large aircraft, a sudden decrease in aerodynamic forces and moments takes place. This situation is more noticeable and dangerous near ground as the small aircraft approaching the ground during landing or take off operations. The lateral position of the small aircraft with respect to the larger one has a great effect, where the lift force could become unsymmetric on both sides of the small wing. This could put the small aircraft into a rolling motion, where it could be deviated from its flight path during the landing or take off operations, an accident might be the result.

KEY WORDS

Computational Fluid mechanics, Aerodynamics, Flight Mechanics.

---

* Assistant Professor, Aeronautical Engineering Department, Faculty of Engineering, Al-Fateh University, P.O. Box 13154, Tripoli, Libya.

** Assistant Professor, Aeronautical Engineering Department, Faculty of Engineering, Al-Fateh University, P.O. Box 13154, Tripoli, Libya.

1- INTRODUCTION

The aerodynamic characteristics of an aircraft are known to be influenced by ground proximity during takeoff and landing. The extensive research conducted to understand and predict ground effect was motivated mainly by the fact that takeoff and landing are among the most dangerous phases of flight. The flow during these phases is inherently unsteady even if the aircraft is moving at constant velocity. This is attributed to the continuous change in the bound circulation around the wings as the ground is approached causing vorticity to be shed into the wake. Experimental studies of this unsteady phenomenon are extremely difficult. On the analytical side, the problem is too complicated to model a full aircraft; however valuable insight can be obtained by considering the lifting surfaces.

The ground plays an important role in modifying the trajectory of the wake vortex during take off and landing. The ground surface acts as a reflection plane, and the motion of vortex pair is determined not only by the mutual induction of the vortices, but also by the image vortex pair below the ground surface.

Based on Nuhait and Mook [1], Wieselsberger in 1922 was the first to model the effect by placing the image of the real lifting surface below the ground plane, thus automatically satisfying the tangency boundary condition on the ground surface.

Recent improvements in computational facilities and numerical techniques have made it possible to study the unsteady ground effect for airfoils, wings and more realistic geometries. Later, ground effect for three-dimensional configurations was investigated. In 1985 Katz [2] used a vortex lattice method, allowing the wake to deform freely, to investigate the performance of a lifting surface of zero thickness close to ground.

In 1989, Nuhait and Mook [1] used the vortex lattice method to study the unsteady flow past two-dimensional and three-dimensional lifting surfaces moving near a ground plane. In 1992-1993, Nuhait and Zedan [3], modified the vortex lattice method of Nuhait and Mook [1] to obtain results for the unsteady flow past a flat and circular arc approaching the ground. Coulliette and Plotkin [4] investigated the influence of the angle of attack on the normalized lift coefficient of airfoils in steady state ground effect. Issa and Archewski [5] used the modified vertex lattice method of Katz [6] to study the wings in unsteady ground effect, they also made a comparison between steady and unsteady motions [7].

In general the wingtip vortices are known to pose a hazard to following aircraft. The vortex system movement near the ground is influenced by two major factors; the lateral spread inherent in the system and wind drift. The strength of the vortex wake is proportional to the weight and inversely proportional to the forward velocity of the generating aircraft. This implies that the strongest wakes are found behind heavy aircraft during take off or landing. In the first case, the aircraft weighs the most, and in both cases, the airspeed is the least. An aircraft encountering a trailing vortex wake near ground could experience large deviations from its flight path. The

magnitude of the deviations depends upon the strength of the vortex wake encountered.
Through the literature review there is no available study concerning the effect of a hazardous wake left by another large scale aircraft on a small aircraft penetrating this wake near ground. Therefore, in this paper the large aircraft represented by a large wing, while, the small aircraft represented by a small wing, with all aerodynamic surfaces assumed to be of zero thickness are considered. Investigation was done for the small aircraft, as it is entering and flying parallel to the wake left by larger aircraft near ground during aircraft landing operation. The lateral position of the small wing with respect to the large wing center line is assumed to be varied. Changes in lift, induced drag, pitching moment and rolling moment coefficients, are calculated and presented for deferent cases of study.

2- GROUND EFFECT

The interaction of the aircraft with the ground is known in the literature as "ground effect." This phenomenon is also observed in ship motion near a canal wall or near a second ship and in the motion of land-based vehicles.

The ground effect is modelled by placing the image of the real lifting surface below the ground plane, thus automatically satisfying the no penetration boundary condition on the ground surface. Therefore, we add the image of the wing and its wake below the ground and there by making the ground as a plane of symmetry. If the ground is rough and not to be modeled as a plane, then can omit the images and instead place panels on the ground. Fig.(1) shows a schematic representation of wing and its image near the ground.

The evaluations of the aerodynamic lift, drag, and moment coefficients are all based on the proper integration of the pressure coefficient on the lifting surface. In this paper the pressure is obtained through an integral representation based on the potential flow model. The lifting surface theory namely *Panel Method* which is applied numerically by what so called *Vortex Lattice Method,* is the proposed method for aerodynamic calculations. The extension of this method into unsteady aerodynamic regime was done in [8]. In this paper, the study is restricted to low angle of attack.

For an irrotational and inviscid flow, a velocity potential can be defined such that

$$V = \nabla \Phi \tag{1}$$

Where Φ is the velocity potential function, and V is linear velocity. If the free stream Mach number is significantly small, the flow may also be considered incompressible. The principle of mass conservation for an incompressible flow has a form;

$$\nabla . V = 0 \tag{2}$$

Equations (1) and (2) can be combined to yield Laplace's equation for the velocity potential;

$$\nabla \cdot \nabla \Phi \equiv \nabla^2 \Phi = 0 \tag{3}$$

In order to complete the formulation of the problem we need to give proper boundary conditions (*BCs*) on the body surface and its image, at the trailing edge and at infinity.

The first *BC* requires zero normal velocity on the wing surface and the ground plane.

$$\nabla \Phi . \mathrm{n} = 0 \tag{4}$$

where *n* is a unit vector normal to the body and ground plane surfaces, respectively.

Along the wing's trailing edge, the velocity has to be limited in order to fix the rear stagnation line (Kutta-Joukowski condition), therefore;

$$\nabla \Phi < \infty \tag{5}$$

The third *BC* requires that the influence of the wing on the flow field must vanish at large distances from the wing

$$\lim_{r \to \infty} \nabla \Phi = 0 \tag{6}$$

It is also important to note that what so-called Kelvin's condition which states that

$$\frac{d\Gamma_b + d\Gamma_w}{dt} = 0 \qquad \text{for all time t} \tag{7}$$

where the subscripts (b) and (w) stand for body and wake, respectively. Eq. (7) is a form of momentum conservation so that the *Helmholtz* theorem is thus automatically satisfied at each time step.

There are many versions of vortex lattice method available for solving equation (3). The modified Vortex Lattice Method is the proposed method, which is an extension of the classical vortex lattice method [9] for the calculation of the aerodynamic forces on lifting surfaces undergoing complex 3-D unsteady motions.

Katz [6] proposed a technique indicating that steady state flow methods can be extended to treat the time dependent problem with only a few modifications. The modifications includes in this paper are the treatment of condition (7) and the use of the unsteady Bernoulli equation. Therefore, the solution can be reduced to solving an equivalent steady state flow problem, at each time step, so this method is called the time-stepping technique [7].

Vortex rings are used to represent the bound vorticity on the wing and the trailing vorticity in the wake. The proposed method is based on the equivalence between constant doublet panel and vortex ring [7]. Fig. (2) shows schematically wing planform, which is divided into panels, and vortex rings are used as singularity elements. The leading segment of the vortex ring is placed on the panel's quarter-chord line and the control point is at the center of the three-quarters chord line. The normal vector $\boldsymbol{n}$ is defined at this point too, which falls at the center of the vortex ring. A positive Γ is defined here according to the right-hand rotation rule.

The lifting surface is divided into panels or elements; vortex rings for the wing, its image and the wake are used as singular elements. The ground influence is represented by image singularities, which are the reflection of the real wing in the ground plane.

When we treat time-dependent motions of an airplane, a selection of frame systems becomes very essential. Two frames are used, one is an inertial (X,Y,Z) fixed to an undisturbed air and the other is fixed to the body (x,y,z) frame of reference. It is usually useful to describe the unsteady motion of the body on which the zero normal flow (*BC*(4)) is applied in the body frame of reference. The motion of this frame is then prescribed in the inertial frame and is assumed to be known. However, the *BC*(4) in this frame becomes

$$\nabla\Phi.n - V_f.n = 0 \tag{8}$$

where V_f is the kinematic velocity as viewed from the inertial frame. Kutta condition (5) and the equation (7) are satisfied by closed vortex representation.

The velocity of the control point is computed according to the relationship for a rigid body;

$$V_f = V_o + \Omega \times r + \mathrm{v_{ref}} \tag{9}$$

where $V_o = (\dot{X}_o, \dot{Y}_o, \dot{Z}_o)$ is the velocity of the origin of (x,y,z) frame, r = (x,y,z) is the position vector, Ω is the rate of rotation of the body's frame of reference, and $\mathrm{v_{ref}} = (\dot{x}, \dot{y}, \dot{z})$. In general, Euler angles are used to define the spatial orientation of the wing in which their derivatives can be used to compute Ω. In the present paper $\Omega = 0$.

Since the wake is dependent upon the motion history, a proper wake model has to be constructed. Roll up and velocity computation are performed in inertial frame of reference, where momentary boundary conditions are imposed in local frame. The wake panels node points (X,Y,Z) are transported by local velocity (U,V,W) induced by body and wake. The displacement at each time step is;

$$\begin{Bmatrix} \Delta X \\ \Delta Y \\ \Delta Z \end{Bmatrix} = \begin{bmatrix} U \\ V \\ W \end{bmatrix} \Delta t \tag{10}$$

Concluding, the steady state solution technique can be updated to treat unsteady flows. The first step is to compute the influence matrix A_{ij}, where A_{ij} is the normal component of the velocity at the control point of element *i* generated by the unit circulation around the vortex segments enclosing element *j* and its image. Since only a half wing is considered, the influence of the other half wing, its image and wake has to be accounted for. At the start of the motion *BC*(4) becomes;

$$\sum_{j=1}^{N} A_{ij}\Gamma_j = RHS_j \tag{11}$$

where $A_{ij} = [(u,w)_{ij} + (u,w)_{ij}^{image}].n_i$, $i = 1,2,....,N$, where N is the number of elements and Γ is the circulation around the vortex segments enclosing element j and *RHS* is the right hand side vector. The *RHS* vector is defined as :

$$RHS_J = -((U+u_w)\sin\alpha + w_w\cos\alpha)_J \tag{12}$$

Where α is the angle of attack. When the circulation distribution Γ_j after the solution of equation (11) is obtained, the difference in pressures a cross the lifting surface is computed at each control point. The pressure can be determined from unsteady Bernoulli equation, written either in body frame of reference or in the inertial frame. In the inertial frame this equation is

$$\frac{p_\infty - p}{\rho} = -V^2 + \Phi_t \tag{13}$$

where $V^2 = \Phi_x^2 + \Phi_y^2 + \Phi_Z^2$, P is the pressure and ρ is the air density. The pressure difference is defined as

$$\nabla P = P_l - P_u$$

$$= \rho\left[\left(\frac{V^2}{2}\right)_u - \left(\frac{V^2}{2}\right)_l + \left(\frac{\partial\Phi}{\partial t}\right)_u - \left(\frac{\partial\Phi}{\partial t}\right)_l\right] \tag{14}$$

According to [9], tangential velocities due to the wing vortices can be approximated as;

$$\pm\frac{\delta\phi}{\delta\tau_i} = \frac{\Gamma_{ij} - \Gamma_{i-1,j}}{2\Delta c_{ij}} \quad , \pm\frac{\delta\phi}{\delta\tau_j} = \frac{\Gamma_{ij} - \Gamma_{i,j-1}}{2\Delta b_{ij}} \tag{15}$$

where $\pm$ represents the upper and lower surfaces and Δc_{ij} and Δb_{ij} are the panel lengths in the *x*-th and *y*-th directions, respectively. Similarly, τ_i and τ_j are the panel tangential vectors in the proper directions.

The velocity potential time derivative is obtained by using the relation

$$\pm\frac{\delta\phi_{ij}}{\delta t}=\pm\frac{\delta}{\delta t}\frac{\Gamma_{ij}}{2} \tag{16}$$

Thus, substituting the terms (15) and (16) into the Eq. (14) one obtains

$$\Delta p_{ij}=\rho\,(U+u_w\,,\,V+v_w\,,\,W+w_w\,)_{ij}\,.\left(\vec{\tau}_i\,\frac{\Gamma_{ij}-\Gamma_{i-1,j}}{\Delta c_{ij}}+\vec{\tau}_j\,\frac{\Gamma_{ij}-\Gamma_{i,j-1}}{\Delta b_{ij}}\right)+\rho\,\frac{\delta}{\delta t}\Gamma_{ij} \tag{17}$$

where (u_w , v_w, w_w) are velocity components induced by the wake vortices, and the undisturbed flow velocity is $U_\infty = (U, V, W)$.

To obtain the loads, the difference of pressure is multiplied by the area of the panel to produce the force on the panel, the panel forces and their moments are added up and the resultants are resolved into lift, drag, pitching moment etc.

For simplicity of the calculation of the induced drag, we limit the motion of the lifting surface in such a way that it moves forward along a straight line without sideslip. The induced drag is the force component parallel to the flight direction and each panel contribution is given by;

$$\Delta D_{ij}=-\,\rho\,(\,w_{ind}+w_w\,)_{ij}\,.\,(\,\Gamma_{ij}-\Gamma_{i\text{-}1,j})\,\Delta b_{ij}+\,\rho\,\frac{\delta}{\delta t}\Gamma_{ij}\;\;.\,\Delta S_{ij}\sin\alpha_{ij} \tag{18}$$

where α_{ij} is the panel's angle of attack, w_{ind} is downwash induced by wing's streamwise vortices, and w_w is downwash induced by wake's streamwise vortices.

The lift, drag and pitching moment coefficients can be computed as follows

$$C_L=\frac{2}{US}\sum_{i,j}S_{ij}\left(\frac{\Gamma_{ij}-\Gamma_{i-1,j}}{\Delta c_{ij}}+\frac{1}{U}\frac{\delta}{\delta t}\Gamma_{ij}\right) \tag{19}$$

$$C_D=\frac{2}{U^2S}\sum_{i,j}S_{ij}\left(-\frac{w_{ind}+w_w}{\Delta c_{ij}}.(\Gamma_{ij}-\Gamma_{i-1,j})+\frac{\delta}{\delta t}\Gamma_{ij}\sin\alpha_{ij}\right) \tag{20}$$

$$C_{m25}=C_L\frac{x_{25}}{c}-\frac{2}{USc}.\sum_{i,j}S_{ij}x_{ij}\left(\frac{\Gamma_{ij}-\Gamma_{i-1,j}}{\Delta c_{ij}}+\frac{1}{U}\frac{\delta}{\delta t}\Gamma_{ij}\right) \tag{21}$$

where S_{ij} is the panel area, x_{ij} and x_{25} are coordinates of the panel quarter-chord and the wing quarter-mean aerodynamic chord, and c is the wing mean aerodynamic chord, respectively. The difference $\Gamma_{ij}-\Gamma_{i\text{-}1,j}$ represents the strength of panel bound vortex, which is placed along the local panel quarter chords. If the panel is at the wing leading edge (i =1) then $\Gamma_{i\text{-}1,j}=0$

4- INTERACTION BETWEEN TWO AERODYNAMIC SURFACES

The interaction between small aircraft and vortex system generated by another much larger aircraft is investigated. A simple wake model can be developed using this vortex system. The model used, is based on the assumption that the effect of flow separation in the resulting flow fields is negligible. In this study, a large wing represents the large aircraft, and a small wing represents the small aircraft are used, with all aerodynamic surfaces assumed to be of zero thickness. Investigation was done for the small aircraft, as it is entering and flying parallel to the wake left by larger aircraft in cruise flight (far of ground) and near ground during aircraft landing operation. The lateral position of the small wing with respect to the large wing centerline is assumed to be varied. Changes in lift, drag, pitching moment and rolling moment coefficients, are calculated and presented for different cases of study.

The larger aircraft represented by its tapered wing is assumed to have landing configuration in all cases of study. The aircraft lift coefficient was set to $C_L \approx 1.54$, representing a landing configuration. The aspect ratio, taper ratio, root chord and sweep back angle are 8.55, 0.35, 4.7 m, and, 24 degrees, respectively.
The small aircraft is represented by its moderate tapered wing of aspect ratio, taper ratio, root chord and sweep back angle, 8.5, 0.676, 1.626 m, and, 3 degrees, respectively. The lift coefficient was set to ≈ 1.02, representing the aircraft landing configuration. The separation (Δx, Δy, Δz) distances are very important . In this investigation only the parameter Δy will be varied as shown in Fig.(4).

5- RESULTS AND DISCUSSION

The method described above has been programmed and run on computer. To get a feel for the program performance, it was run for a thin rectangular wing far off and near to ground with nondimensional time step value of 0.1 and an angle of attack α = 5 degrees. Fig.(4), shows the transient lift coefficients obtained near and far off ground. As can be seen the transient lift coefficient seems to increase near the ground. Finally, both curves increase monotonically with time towards an asymptotic (unity) value.

The numerical solution for the present model is started as initially steady-state problem. The magnitude of the interaction in terms of the aerodynamic coefficients with the nondimensional time *U*T/C* (where C is the larger aircraft wing chord) is presented in the following figures. In this study, a value of 0.2 has been chosen for the nondimansional time step [6]. The numerical simulation is started at t = 0, the smaller aircraft was at large distance behind and parallel to the larger aircraft. As the simulation started, a vortex sheet is generated by the larger aircraft; this sheet is allowed to roll up and deformed into its free position. When the steady state accomplished, the small aircraft enters the wake left by the large aircraft. These analyses were done for several lateral separations (Δy) near ground.

The simulation was performed for the small aircraft near the ground with Δy =0, that is its centerline lies at the large wing centerline; with landing configuration for which (C_L =

1.02) was considered. Due to ground effect, simulation shows higher lift coefficient for both aircrafts ($C_L \approx 1.65$, for large aircraft and $C_L \approx 1.13$, for small aircraft) as compared to no ground effect. These values are function of the aircrafts height above the ground. In fact, the lift coefficient is inversely proportional to aircraft height above the ground. In this study, the height (h) of large aircraft above the ground is equal to 0.6 of its wing span, while the height of small aircraft above ground is 0.4 of large aircraft wing span.

The effect of the aerodynamic interaction near ground on lift of the small aircraft is shown in Fig. (5), this indicates that as the smaller aircraft enters the wake, its lift coefficient increases due to the up wash of the large wing/wake vortex system. But as the aircraft went deep inside the wake, the down wash is prevailing in that area reducing its lift. The ground effect has noticeable and great influence on the lift, the increase of the lift at the beginning of the wake encountered by the small aircraft, and the drop as the aircraft goes deep into the wake, are much more than the ones when ground effect not considered. This implies that the problem is much dangerous near the ground and the inclusion of ground effect in the aerodynamic calculations is very important and necessary for any accurate and successful model.

The drag coefficient history during this operation is presented in Fig.(6). At the beginning, the induced drag has its steady-state value, however, the drag value near the ground is less than its value with no ground effect, due to decrease of induced downwash near the ground. It is seen that, as the small aircraft enters and sinks in to the wake, the induced drag value increase for both cases, due to the increase of induced down wash.

Again, the pitching moment coefficient of Fig.(7), in principle, follows trends similar to the lift coefficient in Fig. (5).

The rolling moment is shown in Fig.(8), because small aircraft was flying at the larger aircraft centerline, again, the rolling moment has zero value for both cases as expected.

The previous simulation is performed for two more different cases. The small aircraft (with landing configuration) flight path was shifted into the right of the larger aircraft centerline (Fig.(9)), i.e., first, its wing centerline lies at the right tip of the large wing. Second, its wing left tip lies at the right tip of the large wing. Therefore, the horizontal separation (Δy) has two values of b_1 and b_1+b_2, where b_1 and b_2 are the large and small aircraft's wing half span, respectively.

Fig.(10), shows the results of lift coefficients for the two positions of the small aircraft wing. In both cases the lift coefficient experience a drop in its value but not as much as when the small aircraft is flying in the centerline of the large one (Δy = 0). In fact, as the separation increases, the difference between the maximum and minimum value of the lift coefficient for both cases decreases, that is due to the fact that, the directions of lift on both sides of wing are opposite, therefore, its absolute value decreases.

Fig. (11), shows the time history of the drag, it can be seen from both figures, as the aircraft changes its position and as the lateral distance increases, the drag decreases and has a negative value as the ground effect is considered, that means, it reverses its direction. This makes the aircraft move faster than it was; this is rather surprising and not expected. However this trend takes a very short time, and may not affect the motion.

Fig. (12), below shows the time history of the pitching moment coefficients, in principle, it follows trends similar to the lift coefficient in Fig. (10) for both cases.

The rolling moments history for these two situations, is shown in Fig.(13). It is seen that as the small aircraft varied its lateral position to a distance of ($\Delta y = b_1$), behind the right wing tip of the large wing, the rolling moment changes its value form zero (positive anti-clockwise), and starts to increase due to the differences between the lift on both sides of small aircraft wing. Due to large wing tip vortex which is rotating anti-clockwise, the right part of the small aircraft wing will have more lift ($\Delta y = b_1$), than left wing, therefore, the small aircraft will experience positive rolling moment. Its value is increased near ground due to ground effect. However, as the separation increases ($\Delta y = b_1+b_2$), with no ground effect, the rolling moment has negative value (clock-wise), because the left part of small aircraft wing has more lift than the right part. In contrary, this is not the case with ground effect, because at this position, the left part of the small wing is flying in the wake and under ground effect, the net lift on the left part is less than that on the right part, so that, a positive rolling moment will result.

6- CONCLUSIONS

A numerical model has been developed to investigate the interaction between small aircraft represented by a small wing, and vortex system generated by another much larger aircraft represented by a large wing. A simple wake model can be developed using this vortex system. The model used, is based on the assumption that the effects of flow separation in the resulting flow fields was negligible. Investigation was done for the small aircraft, as it is entering and flying parallel to the wake left by larger aircraft near ground during aircraft landing operation. The effect of the ground is simulated by placing the plate image below ground surface. However, the wake is allowed to deform and roll up into its natural force free position, which is calculated as part of the solution.

The ground has a significant effect on the wake; the wake has a noticeable influence on the aerodynamic coefficients. Its inclusion is important and essential in the case of aircraft take off and landing, as a light aircraft is passing through a strong wake left behind by a larger aircraft at congested airports or when an aircraft is flying closely to another in the air.

A case study shows that, as the small aircraft enters the wake left by a large aircraft, a sudden change in aerodynamic forces and moments takes place. This situation is more noticeable as the small aircraft is approaching the ground during landing operation due to ground effect. Also, the lateral position of the small aircraft with respect to the larger one has a great effect, where the lift force could become asymmetric on the wing, this could put the small aircraft into a rolling motion, in which the aircraft would deviate from its flight path during the landing operation. For more feasible results, a control surface could be incorporated into the small aircraft model.

As the small aircraft enters the wake of a large aircraft near ground, its lift decreases partially, hence it may loose its altitude, this problem is more dangerous when aircraft height decreases below its wing span during aircraft landing or take off. Also, its rolling moment may change its sign as the investigation shows. A structural damage in aircraft components such as landing gears etc. could happen. The flight path could be disturbed, this could change the landing point on the runway or the aircraft might go out of the runway. In all cases, a fatal accident might occur.

For an airport with multiple runways, one solution to wake problem, is to reserve one runway for small aeroplanes, so that, the interference problem could be reduced with a condition that no high wind drift occurred.

Finally, the full model of unsteady aerodynamics in ground effect of lifting surfaces has not been completed yet. More investigations have to be done to study this effect on the other aerodynamic coefficients, stability derivatives, etc. The investigation could be extended to study the effect of this phenomenon on aircraft flight dynamics behavior, structural dynamics, etc.

7- REFERENCES

1. Nuhait, A.O. and Mook, D.T., "Numerical Simulation of Wings in Steady and Unsteady Ground Effects", J Aircraft, 26, pp1081-1089, (1989).
2. Katz, J. " Calculation of Aerodynamic Forces on Automotive Lifting Surfaces" J. of Fluid Eng, 26, pp 438-443, (1985).
3. Nuhait, A.O. and Zedan, M.F., "Numerical Simulation of Unsteady Flow Induced by a Flat Plate Moving Near Ground", J Aircraft, 30, pp 611-617, (1993).
4. Coulliette, C. and Plotkin, A., "Aerofoil Ground Effect Revisited " Aeronautical J, pp 65-74, (1996).

5- Issa, S.M. and Arczewski, K.P., "Wings in Unsteady Ground Effect" Second International Seminar on Recent Research and Design Progress in Aeronautical Engineering and its Influence on Education, Warsaw, Poland, pp 155-160, (1996).

6. Katz, J. and Plotkin, A. " Low-speed aerodynamic: from wing theory to panel Methods" McGraw-Hill, (1991).

7- Issa, S.M. and Arczewski, K.P., " Wings in Steady and Unsteady Ground Effects" Canadian Aeronautics and Space Journal, Vol. 44, No. 3, (1998).

8. Levin D. and Katz J., " Vortex-Lattice Method for the Calculation of the Nonsteady Separated Flow over Delta Wings" J Aircraft, Vol. 18 No. 12, PP 1032-1037, (1981).

[9]- Bertin, J.J. and Smith M.L., "Aerodynamics for Engineers", Practice-Hall Inter., London (1989).

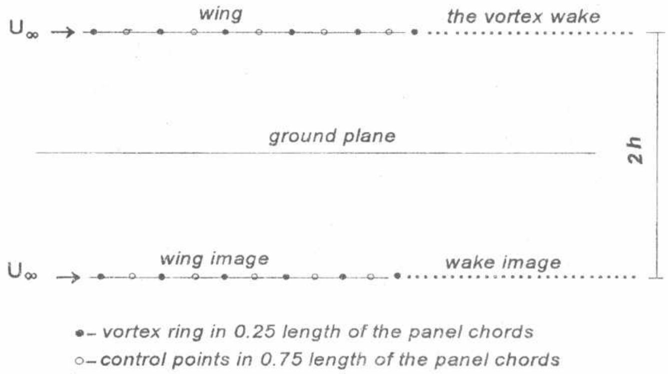

Fig. (1) The wing and its image near the ground

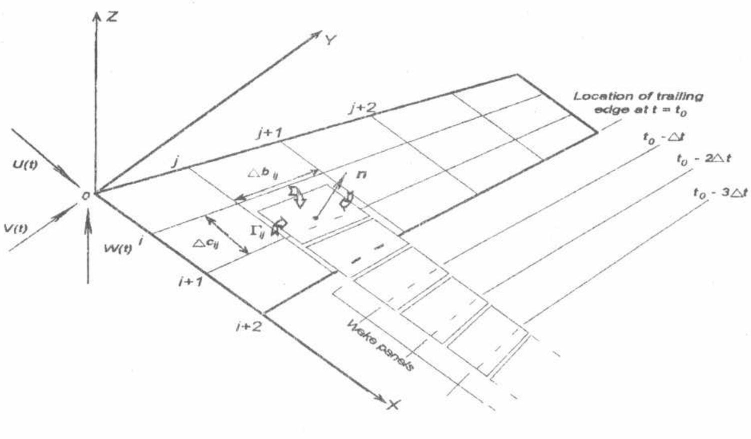

Fig. (2) Nomenclature for the unsteady motion of a thin wing along a predetermined path

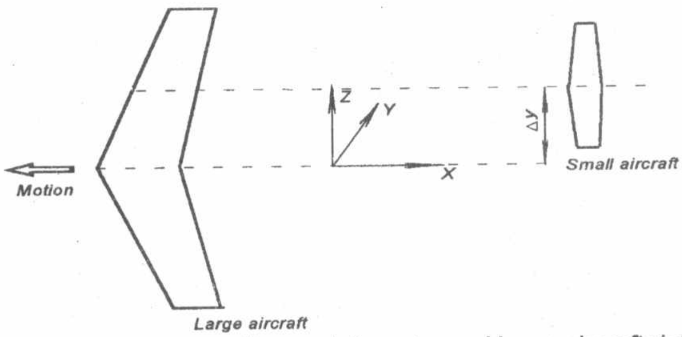

Fig.(3) Small aircraft wing centerline variations toward large aircraft right wing tip

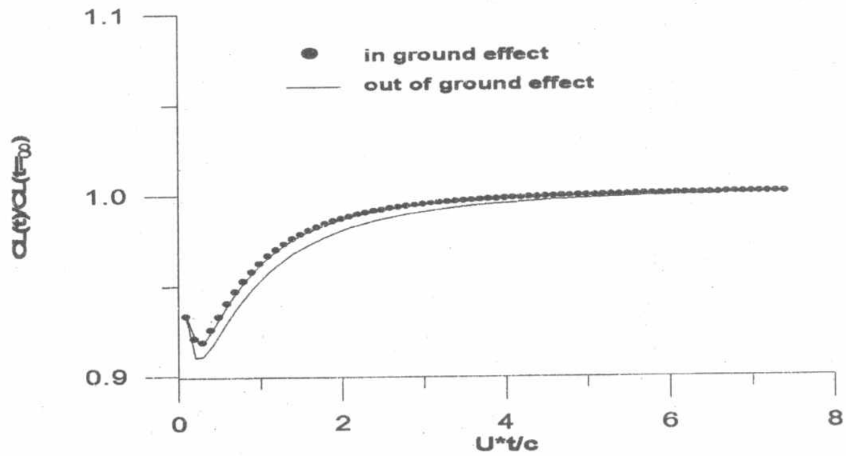

Fig.(4) Effect of ground effect on nondimensional transient lift of a thin rectangular wing.

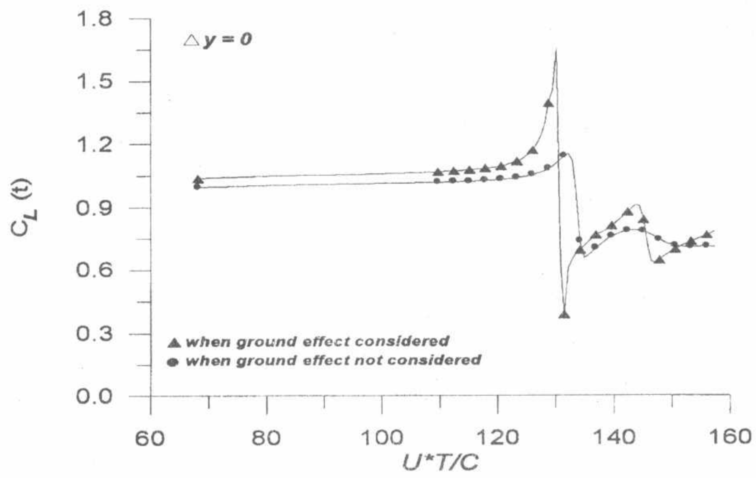

Fig. (5) Lift coefficient for small aircraft (landing configuration)

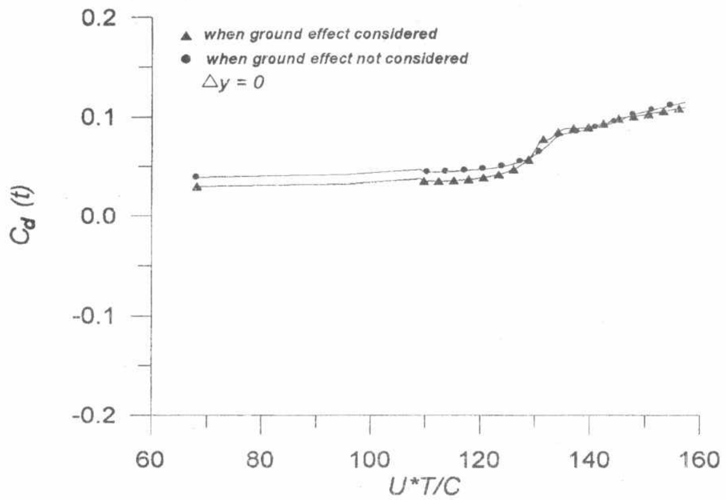

Fig.(6) Drag coefficient for small aircraft (landing configuration)

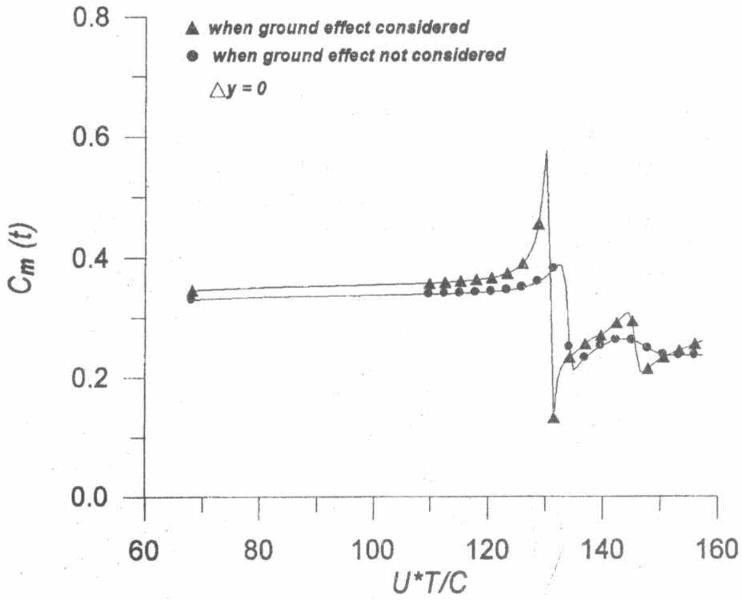

Fig.(7) Pitching moment coefficient for small aircraft (landing configuration)

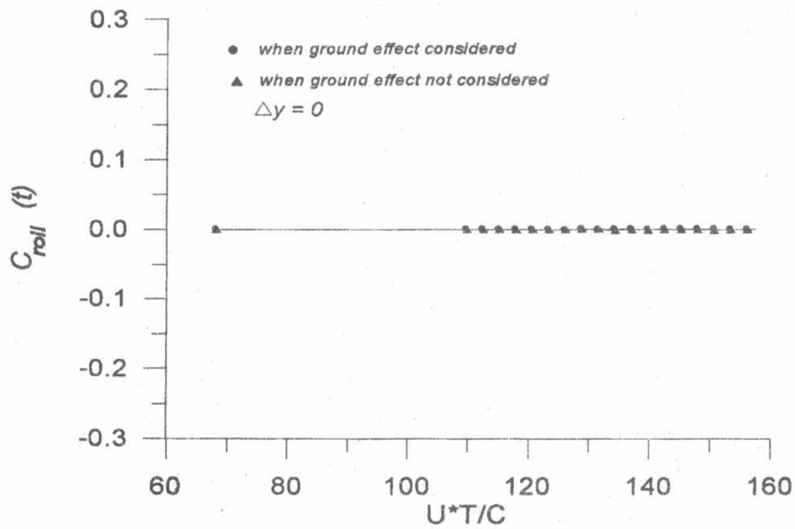

Fig.(8) Rolling moment coefficient for small aircraft (landing configuration)

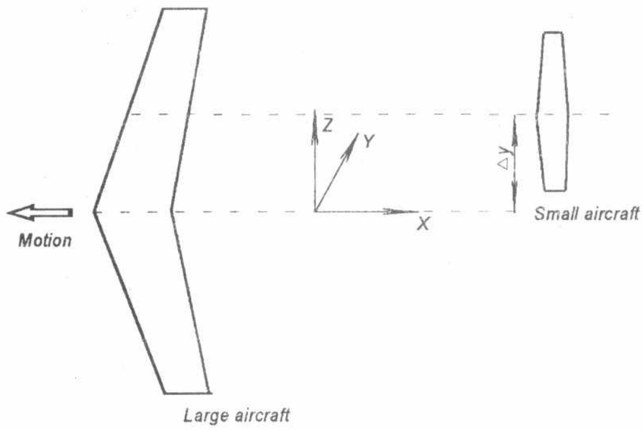

Fig.(9) Small aircraft wing centerline shifted toward large aircraft right wing tip

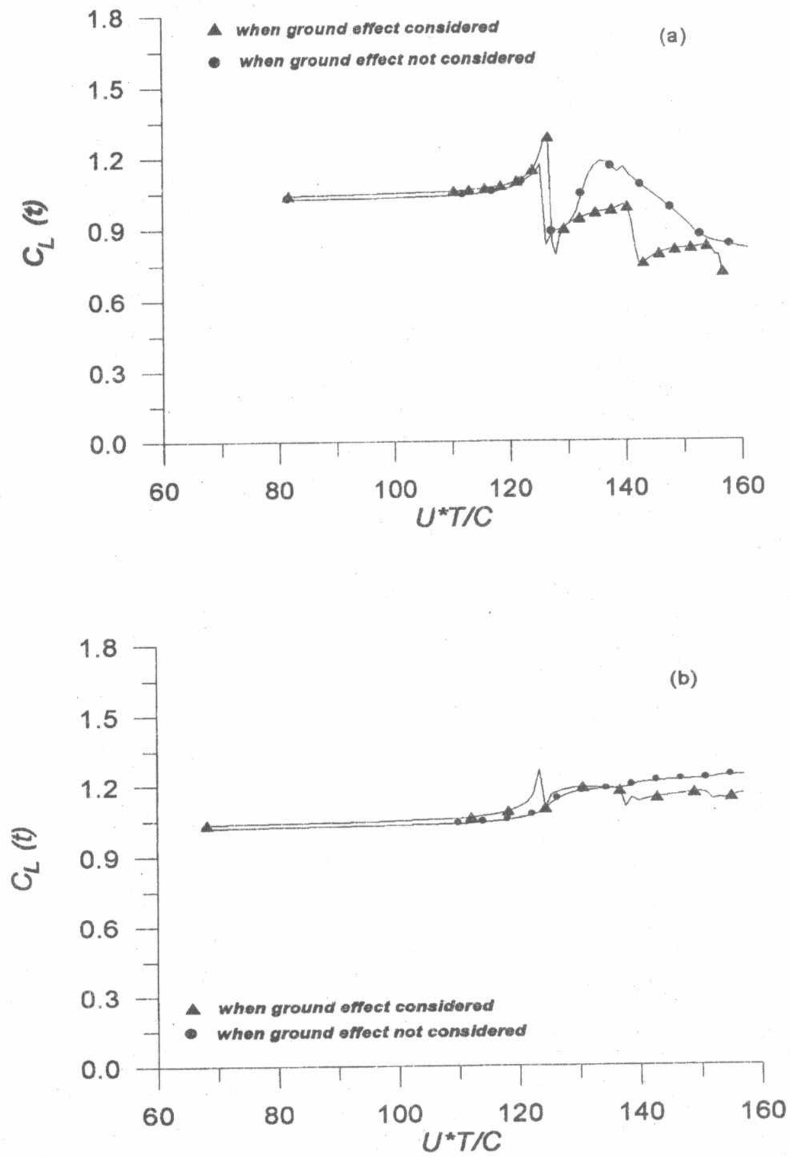

Fig.(10) Lift coefficient for small aircraft when flight path shifted (landing configuration)
(a) $\Delta y = b_1$ (b) $\Delta y = b_1 + b_2$

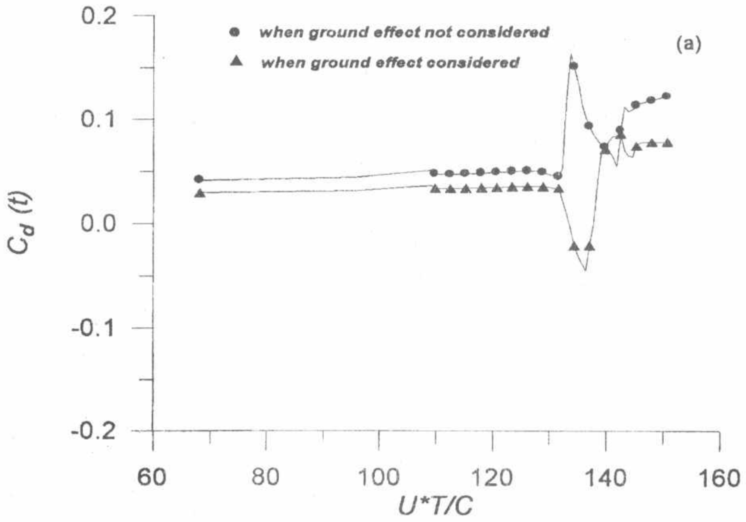

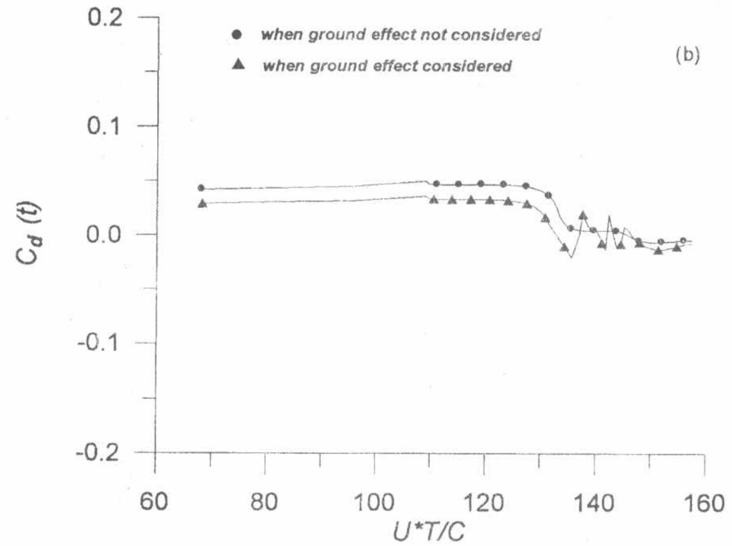

Fig.(11) Drag coefficient for small aircraft when flight path shifted (landing configuration)
(a) $\Delta y = b_1$ (b) $\Delta y = b_1 + b_2$

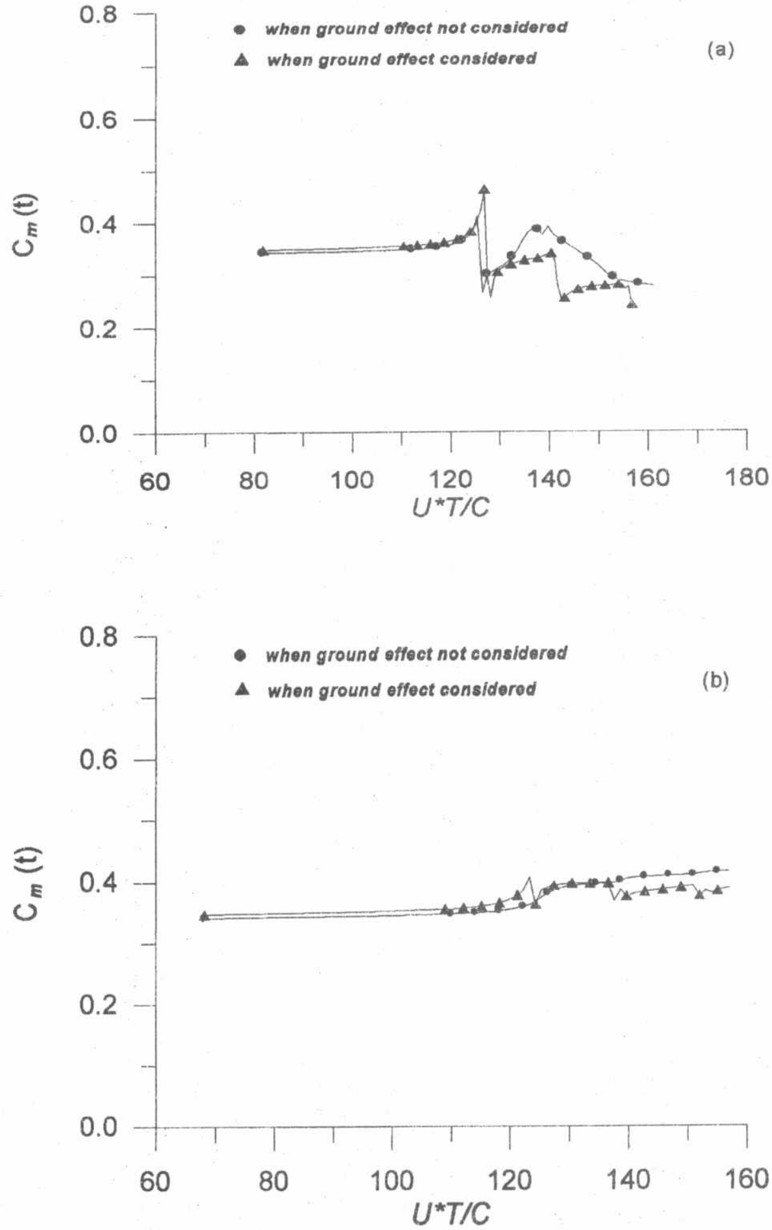

Fig. (12) Pitching moment coefficient for small aircraft when flight path shifted (landing configuration), (a) $\Delta y = b_1$ (b) $\Delta y = b_1 + b_2$

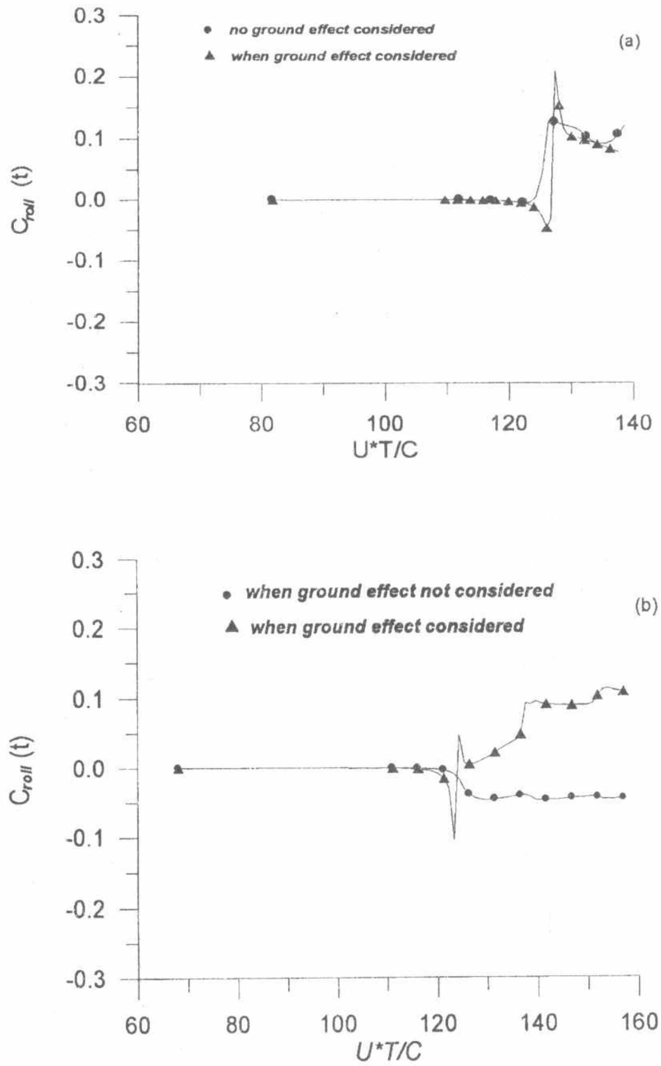

Fig.(13) Rolling moment coefficient for small aircraft when flight path shifted (landing configuration), (a) $\Delta y = b_1$ (b) $\Delta y = b_1 + b_2$